Lewis Acid Properties of Tris(pentafluorophenyl)borane. Structure and Bonding in L−B(C_6F_5)$_3$ Complexes[⊥]

Heiko Jacobsen,[†] Heinz Berke,*[,†] Steve Döring,[‡] Gerald Kehr,[‡] Gerhard Erker,*[,‡] Roland Fröhlich,[‡,§] and Oliver Meyer[‡,§]

Anorganisch-Chemisches Institut, Universität Zürich-Irchel, Winterthurerstrasse 190, CH-8057 Zürich, and Organisch-Chemisches Institut, Universität Münster, Corrensstrasse 40, D-48149 Münster

Received December 21, 1998

A variety of donor adducts of tris(pentafluorophenyl)borane were experimentally generated by reaction of a Lewis base with an excess of B(C_6F_5)$_3$ in pentane. In this way, nitrile complexes (C_6F_5)$_3$B·NCR (R = CH_3 **1a**, *p*-CH_3−C_6H_4 **1b**, *p*-NO_2−C_6H_4 **1c**), isonitrile complexes (C_6F_5)$_3$B·CNR (R = $C(CH_3)_3$ **3a**, $C(CH_3)_2CH_2C(CH_3)_3$ **3b**, 2,6-$(CH_3)_2$−C_6H_3 **3c**), and the phosphine adduct (C_6F_5)$_3$B·P(C_6H_5)$_3$ (**6**) could be prepared. The compounds were characterized by IR and NMR spectroscopy and by X-ray structure analyses (**1a**, **1c**, **3a**, **3b**, and **6**). Coordination of the nitriles as well as the isonitriles to the neutral Lewis acid leads to a substantial increase in the C≡N bond strength. This is evident from a marked shift of the $\tilde{\nu}_{C\equiv N}$ IR band to higher wavenumbers, and this interpretation is supported by the small but experimentally significant decrease of the C≡N bond length observed by X-ray diffraction. The experimental work is complemented by a density functional study on the model complexes (C_6F_5)$_3$B·L, L = $CNCH_3$, $NCCH_3$, PH_3, CO. A detailed analysis revealed that the bonding in (C_6F_5)$_3$B·L complexes is mainly dominated by electrostatic interaction, which in turn is responsible for the observed structural and spectroscopic changes. In the context of this work, the bonding of the neutral B(C_6F_5)$_3$ Lewis acid is compared to the positively charged organometallic d_0-Cp_3M^+ system (M = Zr, Hf). It was found that electrostatic effects are more pronounced for B(C_6F_5)$_3$ than for the transition metal fragments. The question as to the existence of a nonclassical main group carbonyl complex, (C_6F_5)$_3$B·CO, is addressed.

Introduction

Since boranes are among the prototypes of Lewis acids, the reaction of boron trihalides, e.g. BF_3, with strong electron donors such as NH_3 provides a typical textbook example[1] of interactions between Lewis type acids and bases. According to Pearson's HSAB principle,[2] the two species mentioned above have to be classified both as a hard acid and as a hard base. Elaborating on HSAB theory, we would expect that complexes between a soft acid and a soft base should also lead to stable species. The classical example involving boron-based molecules is the H_3B·CO complex, which has been known for about 60 years[3] and has been under intense scrutiny by both experimentalists[4] and theoreticians.[5] The recent calculations by Bauschlicher and Ricca[6] on the energetics of H_3B·CO are expected to reflect the most accurate results obtained to date.

The question arises whether complexes of hard boron centers and soft bases, like F_3B·CO, might also possess some thermodynamic stability. Initial attempts to prepare this addition compound by Shepp and Bauer proved unsuccessful;[4c] the authors estimated the bond-forming reaction to be endothermic. It took more than 20 years before Klemperer and co-workers[7] succeeded in recording the microwave spectrum of F_3B·CO they produced by supersonic expansion. Their studies concluded that F_3B·CO is only weakly bound, with an

[⊥] Dedicated to Professor Helmut Werner on the occasion of his 65th birthday.

[†] Universität Zürich-Irchel.

[‡] Universität Münster.

[§] X-ray crystal structure analysis.

(1) (a) Wiberg, N. *Hollemann-Wiberg − Lehrbuch der Anorganischen Chemie*, 91st−100th ed.; Walter de Gruyter: Berlin, 1985; Chapter 3.1.2. (b) March, J. *Advanced Organic Chemistry*, 3rd ed.; John Wiley: New York, 1985; p 227 ff.

(2) (a) Pearson, R. G. *J. Am. Chem. Soc.* **1963**, *85*, 3533. (b) Pearson, R. G. *Science* **1966**, *151*, 172.

(3) Burg, A. B.; Schlesinger, H. I. *J. Am. Chem. Soc.* **1937**, *59*, 780.

(4) (a) Bauer, S. H. *J. Am. Chem. Soc.* **1937**, *59*, 1804. (b) Gordy, W.; Ring, H.; Burg, A. B. *Phys. Rev.* **1950**, *78*, 512. (c) Burg, A. B. *J. Am. Chem. Soc.* **1952**, *74*, 3482. (d) Shepp, A.; Bauer, S. H. *J. Am. Chem. Soc.* **1954**, *76*, 265. (e) McCoy, R. E.; Bauer, S. H. *J. Am. Chem. Soc.* **1956**, *78*, 2061. (f) Bethke, G. W.; Wilson, M. K. *J. Chem. Phys.* **1957**, *26*, 1118. (g) Garabedian, M.; Benson, S. W. *J. Am. Chem. Soc.* **1964**, *86*, 176. (h) Fehlner, T. P.; Koski, W. S. *J. Am. Chem. Soc.* **1965**, *87*, 409. (i) Grotewold, J.; Lissi, E. A.; Villa, A. E. *J. Chem. Soc. A* **1966**, 1038. (j) Fehlner, T. P.; Mappes, G. W. *J. Phys. Chem.* **1969**, *73*, 873. (k) Ganguli, P. S.; McGee, H. A. *J. Chem. Phys.* **1969**, *50*, 4658. (l) Mappes, G. W.; Friedmann, S. A.; Fehlner, T. P. *J. Phys. Chem.* **1970**, *74*, 3307. (m) Pépin, C.; Lambert, L.; Cabana, A. *J. Mol. Spectrosc.* **1974**, *53*, 120. (n) Beach, D. B.; Eyermann, C. J.; Smit, S. P.; Xiang, S. F.; Jolly, W. J. *J. Am. Chem. Soc.* **1984**, *106*, 536. (o) Pradeep, T.; Sreekanth, C. S.; Hedge, M. S.; Rao, C. N. R. *J. Mol. Struct.* **1989**, *194*, 163. (p) Pasternack, L.; Weiner, B. R.; Baronavski, A. P. *Chem. Phys. Lett.* **1989**, *154*, 121.

(5) (a) Umeyama, H.; Morokuma, K. *J. Am. Chem. Soc.* **1976**, *98*, 7208. (b) Bentley, T. W. *J. Org. Chem.* **1982**, *47*, 60. (c) Røeggen, I. *Chem. Phys.* **1992**, *162*, 271. (d) Murakhtanov, V. V. *Zh. Strukt. Khim.* **1992**, *33*, 14. (e) Glendening, E. D.; Streitwieser, A. *J. Chem. Phys.* **1994**, *100*, 2900. (f) Skancke, A.; Liebman, J. *J. Phys. Chem.* **1994**, *98*, 13215. (g) Jonas, V.; Frenking, G.; Reetz, M. T. *J. Am. Chem. Soc.* **1994**, *116*, 8741.

(6) Bauschlicher, C. W., Jr.; Ricca, A. *Chem. Phys. Lett.* **1995**, *237*, 14.

(7) Janda, K. C.; Bernstein, L. S.; Steed, J. M.; Novick, S. E.; Klemperer, W. *J. Am. Chem. Soc.* **1978**, *100*, 8074.

10.1021/om981033e CCC: $18.00
Publication on Web 04/09/1999

unusually long B−C bond distance. The experimental findings could later be reproduced in the theoretical calculations by Bauschlicher and Ricca,[6] and others.[5g,8] Very recently, Sluyts and van der Veken[9] were able to measure the enthalpy of formation for $F_3B{\cdot}CO$, thus confirming and quantifying the earlier results.

Those developments spawned our interest to investigate the Lewis acid properties of a related molecule, which in the past decade "emerged from relative obscurity to a position of prominence", namely tris(pentafluorophenyl)borane,[10] B(C$_6$F$_5$)$_3$. One of the discoveries leading to the modern chemistry of B(C$_6$F$_5$)$_3$ was certainly its effectiveness as an initiator of olefin polymerization, in combination with group IV metallocene alkyls.[11]

To the best of our knowledge, only a few donor adducts of B(C$_6$F$_5$)$_3$ are structurally characterized in the literature. Besides O-carbonyl adducts of C$_6$H$_5$C(O)R, R = H, Me, OEt,[12] and N(^{i}Pr)$_2$,[12b] and one N-imidazole complex,[13] there exist structures of two phosphine adducts of tris(pentafluorophenyl)borane, (C$_6$F$_5$)$_3$B·PH$_3$[14] and (C$_6$F$_5$)$_3$B·PH$_2$C(CH$_3$)$_3$.[15] Here we will describe the synthesis and crystal structure analysis of three types of donor adducts of B(C$_6$F$_5$)$_3$, namely isonitrile complexes (C$_6$F$_5$)$_3$B·CNR, nitrile complexes (C$_6$F$_5$)$_3$B·NCR, and the phosphine adduct (C$_6$F$_5$)$_3$B·P(C$_6$H$_5$)$_3$. The experimental work is complemented by theoretical calculations on the model complexes (C$_6$F$_5$)$_3$B·L, L = CNCH$_3$, NCCH$_3$, PH$_3$, CO. The calculations are based on density functional theory[16] and are implemented to provide a deeper understanding into the nature of the Lewis type donor adducts.

The goal of the present study is two fold. As mentioned earlier, we want to investigate and classify the Lewis acidity of B(C$_6$F$_5$)$_3$ in comparison with prototypes of soft and hard acids, BH$_3$ and BF$_3$, but we are also interested in the donor behavior of classical π acceptor ligands in transition metal chemistry, such as CO and isonitriles. When these molecules coordinate to the tris(pentafluorophenyl)borane fragment, one might anticipate π contributions to be of minor importance only. In a way, donor adducts such as (C$_6$F$_5$)$_3$B·CO might be compared to the class of homoleptic metal carbonyl cations,[17] complexes that have been termed "nonclassical". Carbonyl stretches in these compounds are found at higher wavenumbers than those of free CO, often by more than 100 cm^{-1}. Goldmann and Krogh-Jespersen[18] have analyzed the origin of this $\tilde{\nu}_{CO}$ shift and found that electrostatic effects, and not an enhanced σ donation, are the responsible factors. It has been further shown that the M−CO bond in cationic transition metal carbonyls has a reduced π component compared to that of neutral complexes.[19] Within this context, we want to address the question of whether (C$_6$F$_5$)$_3$B·CO might indeed be considered a nonclassical main group carbonyl complex and extend this problem to include other representative ligands used in transition metal chemistry, such as phosphines, isonitriles, and nitriles.

Results and Discussion

Experimental Studies. Tris(pentafluorophenyl)borane was prepared for this study by a variation of the procedure originally developed by Stone, Massey, and Park.[20] Pentafluorobromobenzene was converted to pentafluorophenyllithium at low temperature. The potentially explosive C$_6$F$_5$Li reagent was then reacted with BCl$_3$ under carefully controlled reaction conditions to give pure B(C$_6$F$_5$)$_3$, isolated in ca. 40% yield after precipitation from pentane.

In the course of this study we have prepared and isolated three nitrile adducts **1a**−**c** and three isonitrile addition products **3a**−**c** of the organometallic Lewis acid tris(pentafluorophenyl)borane. We had previously shown by the NMR method of Childs et al.[21] that B(C$_6$F$_5$)$_3$ is a slightly stronger Lewis acid than BF$_3$. On the respective scale, where BBr$_3$ is assigned a relative Lewis acid strength of 1.0, BCl$_3$ (0.77) and SnCl$_4$ (≈0.5) are framing B(C$_6$F$_5$)$_3$, to which a value of 0.72 was assigned.[22] Therefore, it was not surprising that the Lewis acid B(C$_6$F$_5$)$_3$ rapidly forms an adduct upon treatment with acetonitrile. The reaction was carried out in a way that slightly less than 1 molar equiv of acetonitrile was added to a solution of B(C$_6$F$_5$)$_3$ in pentane at room temperature. Under these conditions the adduct formation is quite rapid, and the H$_3$C−C≡N−B(C$_6$F$_5$)$_3$ addition product **1a** precipitates from the solution. The adduct **1a** was isolated in >95% yield. It shows a ^{11}B NMR signal at δ −10.3 ppm (in benzene-d_6), which is as expected for tetracoordinated boron in an organic environment. Compound **1a** exhibits a characteristic IR band at $\tilde{\nu}$ = 2367 cm^{-1}, which is to be compared with the respective IR features of the free, uncoordinated acetonitrile molecule [$\tilde{\nu}$ = 2292 cm^{-1} (CH$_3$−C≡N combination) and $\tilde{\nu}$ = 2253 cm^{-1} (C≡N stretch)].[23]

(8) Luken, W. L.; Sieders, B. A. B.; Blake, G. A. *Chem. Phys.* **1982**, *92*, 255.
(9) (a) Sluyts, E. J.; van der Veken, B. J. *J. Am. Chem. Soc.* **1996**, *118*, 440. (b) van der Veken, B. J., Sluyts, E. J. *J. Mol. Struct.* **1995**, *349*, 461.
(10) Piers, W. E.; Chivers, T. *Chem. Soc. Rev.* **1997**, *26*, 345.
(11) Yang, X.; Stern, C. L.; Marks, T. J. *J. Am. Chem. Soc.* **1994**, *116*, 10015.
(12) (a) Parks, D. J.; Piers, W. *Am. Chem. Soc.* **1996**, *118*, 9440. (b) Parks, D. J.; Piers, W.; Parvez, M.; Atencio, R.; Zaworotko, M. J. *Organometallics* **1998**, *17*, 1369.
(13) Röttger, D.; Erker, G.; Fröhlich, R.; Kotila, S. *J. Organomet. Chem.* **1996**, *518*, 17.
(14) Bradley, D. C.; Hursthouse, M. B.; Motevalli, M.; Zheng, D. H. *J. Chem. Soc., Chem. Commun.* **1991**, 7.
(15) Bradley, D. C.; Harding, I. S.; Keefe, A. D.; Motevalli, M.; Zheng, D. H. *J. Chem. Soc., Dalton Trans.* **1996**, 3931.
(16) (a) Ziegler, T. *Pure. Appl. Chem.* **1991**, *28*, 1271. (b) Ziegler, T. *Chem. Rev.* **1991**, *91*, 651. (c) Ziegler, T. *Can. J. Chem.* **1995**, *73*, 743. (d) *Density Functional Methods in Chemistry*; Labanowski, J., Andzelm, J., Eds.; Springer: Heidelberg, 1991. (e) *Density Functional Theory*; Gross, E. K. U., Dreizler, R. M., Eds.; Plenum: New York, 1995. (f) *Chemical Applications of Density Functional Theory*; Laird, B. B., Ross, R. B., Ziegler, T., Eds.; ACS Symposium Series 629; Washington, DC, 1996.
(17) Willner, H.; Aubke, F. *Angew. Chem.* **1997**, *109*, 2506; *Angew. Chem., Int. Ed. Engl.* **1997**, *36*, 2402.
(18) Goldman, A. S.; Krogh-Jespersen, K. *J. Am. Chem. Soc.* **1996**, *118*, 12159.
(19) (a) Ehlers, A. W.; Ruiz-Morales, Y.; Baerends, E. J.; Ziegler, T. *Inorg. Chem.* **1997**, *36*, 5031. (b) Szilagyi, R. K.; Frenking, G. *Organometallics* **1997**, *16*, 4807.
(20) Massey, A. G.; Park, A. J.; Stone, F. G. A. *Proc. Chem. Soc.* **1963**, 212. Massey, A. G.; Park, A. J. *J. Organomet. Chem.* **1964**, *2*, 245. Massey, A. G.; Park, A. J. In *Organometallic Synthesis*; King, R. B., Eisch, J. J., Eds.; Elsevier: New York, 1986; Vol. 3, p 461.
(21) Childs, R. F.; Mulholland, D. L. *Can. J. Chem.* **1982**, *60*, 801, 809. Laszlo, P.; Teston, M. *J. Am. Chem. Soc.* **1990**, *112*, 8750.
(22) Döring, S.; Erker, G.; Fröhlich, R.; Meyer, O.; Bergander, K. *Organometallics* **1998**, *17*, 2183.
(23) (a) Bruce, M. R. M.; Tyler, D. R. *Organometallics* **1985**, *4*, 528. See also: Jordan, R. F.; Dasher; W. E.; Echols, S. F. *J. Am. Chem. Soc.* **1986**, *108*, 1718. (b) Li, L.; Marks, T. J. *Organometallics* **1998,** *17*, 3996.

Single crystals of **1a** suitable for an X-ray crystal structure analysis were obtained by the diffusion method, letting pentane slowly condense into a solution of **1a** in benzene-d_6. The X-ray crystal structure analysis of **1a** confirms the formation of a 1:1 adduct between acetonitrile and $B(C_6F_5)_3$. The two components are connected by means of a strong B−N bond (1.616(3) Å). The boron atom is tetracoordinated. The average length of the B−C(aryl) linkages amounts to 1.629(4) Å. The boron coordination geometry is distorted tetrahedral with average N−B−C(aryl) bonding angles of 104.0(2)° and average C(aryl)-B−C(aryl) angles of 114.3(2)°. In the crystal, the L−B(aryl)$_3$ unit attains a chiral conformation, as is often observed for such borane adducts and also for related triarylborate systems,[25] but this relative orientation of the aryl planes of **1a** at boron is not persistent in solution. In the crystal, the $H_3C^2-C^1\equiv N-$[B] axis is close to linear, with bond angles C2−C1−N (178.9(3)°) and C1−N−B (177.1(2)°) both being close to 180°. The C2−C1 bond length is 1.452(4) Å, and thus in the expected C(sp^3)−C(sp) single bond range. Most noteworthy is the C1−N bond length of **1a**, for which a value of 1.124(3) Å was determined. We had recently carried out a rather accurate crystal structure analysis of the uncoordinated acetonitrile molecule.[26] Crystals for that specific study were obtained on a Laser zone melting apparatus, as developed by Boese et al.,[27] which was connected to a diffractometer. For acetonitrile (α-phase at 208 K) a value of 1.141(2) Å was obtained for the −C≡N triple bond. Thus we note that coordination of acetonitrile to the neutral strong organometallic Lewis acid tris(pentafluorophenyl)borane leads to a measurable strengthening of the −C≡N bond. Structurally this effect is similar in magnitude as observed upon complexation of acetonitrile to the positively charged d_0-configurated organometallic Lewis acid Cp_3Zr^+ ($d_{C\equiv N}$ in the complex $[Cp_3Zr-N\equiv C-CH_3]^+$ **2a**: 1.126(5) Å).[26] We conclude that in both systems, the neutral acetonitrile−$B(C_6F_5)_3$ **1a** and the positively charged acetonitrile−$ZrCp_3^+$ **2a**, the resulting nitrile −C≡N triple bond becomes stronger upon Lewis acid/Lewis base adduct formation. Upon adduct formation in both systems, the crystallographically determined $d_{C\equiv N}$ value decreases and the $\tilde{\nu}_{C\equiv N}$ band shifts considerably to higher wavenumbers [$\Delta\tilde{\nu}$ = +114 cm^{-1} **1a**; +59 cm^{-1} **2a**].

Next we prepared the *p*-methylbenzonitrile/$B(C_6F_5)_3$ adduct **1b**. The compound was isolated in 77% yield and characterized by elemental analysis and NMR and IR spectroscopy. In this case, the IR $\tilde{\nu}_{C\equiv N}$ band is again substantially shifted to higher wavenumbers on going from the free nitrile [$\tilde{\nu}_{C\equiv N}$ = 2227 cm^{-1} (neat)] to the adduct [**1b**: $\tilde{\nu}_{C\equiv N}$ = 2322 cm^{-1}, in KBr, $\Delta\tilde{\nu}$ = +95 cm^{-1}].

We then examined *p*-$O_2N-C_6H_4-C\equiv N-B(C_6F_5)_3$ **1c** and found an increase of the $\tilde{\nu}_{C\equiv N}$ IR band by $\Delta\tilde{\nu}$ = +99 cm^{-1} on going from the free nitrile to the tris(pentafluorophenyl)borane adduct (**1c**: 2334 cm^{-1}). The adduct **1c** was also characterized by X-ray diffraction. The bond lengths and angles of **1c** (see Figure 2) around boron are very similar to those found for **1a** (see above) (**1c**: N6−B7 1.595(3) Å, average B−C(aryl) 1.632(3) Å, average N−B−C(aryl) angle 104.5(2)°, average C(aryl)−B−C(aryl) angle 114.0(2)°). The B7−N6−C5−C43 moiety is linear (angles B7−N6−C5 178.9(2)°, N6−C5−C43 178.3(2)°), and the $C^5\equiv N^6$ bond is again very short at 1.135(3) Å.

The *tert*-butylisocyanide/$B(C_6F_5)_3$ adduct **3a** was analogously prepared by treatment of tris(pentafluorophenyl)-borane with $Me_3C-N\equiv C$ in pentane. The adduct was isolated in 64% yield. Single crystals were obtained by allowing pentane to very slowly condense into a benzene solution of **3a**. The typical ^{11}B NMR chemical shift of the addition product at δ = −21.8 ppm indicates the formation of a tetracoordinate boron species. The coordination of the isonitrile again has caused a distorted

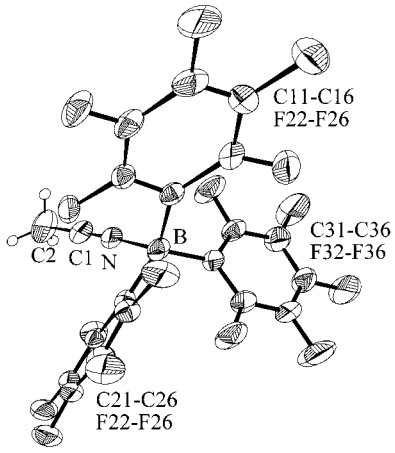

Figure 1. View of the molecular structure of the acetonitrile/$B(C_6F_5)_3$ adduct **1a** in the crystal. Selected bond lengths (Å) and angles (deg): B−N 1.616(3), B−C11 1.639-(4), B−C21 1.625(4), B−C31 1.622(4), N−C1 1.124(3), C1−C2 1.452(4); N−B−C11 102.5(2), N−B−C21 104.0(2), N−B−C31 105.5(2), C11−B−C21 114.9(2), C11−B−C31 115.7(2), C21−B−C31 112.4(2), B−N−C1 177.1(2), N−C1−C2 178.9-(3).

Scheme 1

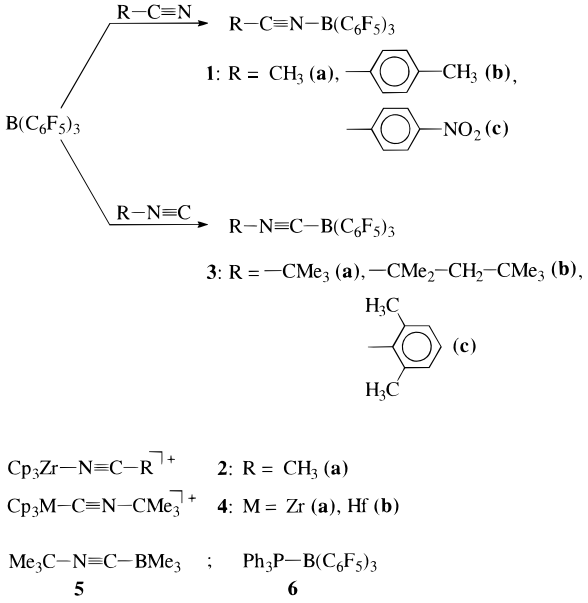

$Cp_3Zr-N\equiv C-R^{]+}$ **2**: R = CH_3 (**a**)

$Cp_3M-C\equiv N-CMe_3^{]+}$ **4**: M = Zr (**a**), Hf (**b**)

$Me_3C-N\equiv C-BMe_3$; $Ph_3P-B(C_6F_5)_3$

5 **6**

(24) Orpen, A. G.; Brammer, L.; Allen, F. H.; Kennard, O.; Watson, D. G.; Taylor, R. J. *Chem. Soc., Dalton Trans.* **1989**, S1.

(25) Ahlers, W.; Temme, B.; Erker, G.; Fröhlich, R.; Fox, T. *J. Organomet. Chem.* **1997**, *527*, 191.

(26) Brackemeyer, T.; Erker, G.; Fröhlich, R.; Prigge, J.; Peuchert, U. *Chem. Ber. Recl.* **1997**, *130*, 899.

(27) Brodalla, D.; Mootz, D.; Boese, R.; Osswald, W. *J. Appl. Crystallogr.* **1985**, *18*, 316. Boese, R.; Nussbaumer, M. In situ Crystallization Techniques. In *Correlations, Transformations and Interactions in Organic Crystal Chemistry*; IUCr Crystallographic Symposia, Vol. 7; Jones, D. W., Katrusiak, A., Eds.; Oxford Science Publications: Oxford, 1994; pp 20−38.

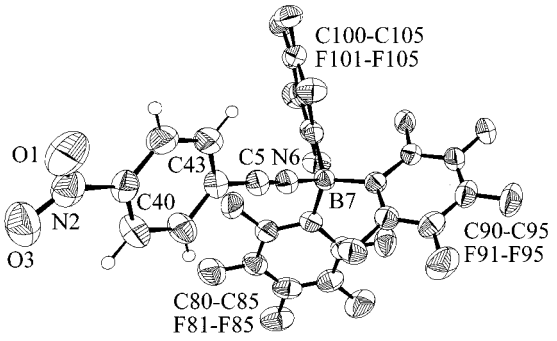

Figure 2. Molecular geometry of **1c** in the crystal. Selected bond lengths (Å) and angles (deg): B7−N6 1.595(3), B7−C80 1.634(3), B7−C90 1.626(3), B7−C100 1.640(3), N6−C5 1.135(3), C5−C43 1.431(3), C40−N2 1.477(3), N2−O1 1.219(3), N2−O3 1.224(3); N6−B7−C80 104.6(2), N6−B7−C90 104.6(2), N6−B7−C100 104.2(2), C80−B7−C90 113.5(2), C80−B7−C100 112.5(2), C90−B7−C100 116.0(2), B7−N6−C5 178.9(2), N6−C5−C43 178.3(2), C40−N2−O1 117.7(2), C40−N2−O3 116.8(2), O1−N2−O3 125.4(2).

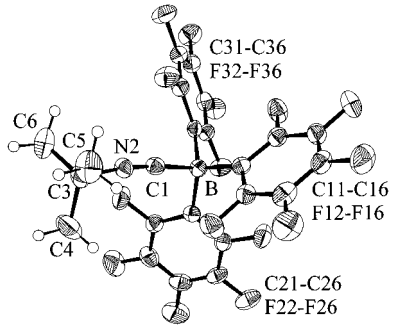

Figure 3. Molecular structure of the Me$_3$C−N≡C/addition product **3a**. Selected bond lengths (Å) and angles (deg): B−C1 1.624(4), B−C11 1.632(4), B−C21 1.644(4), B−C31 1.623(4), C1−N2 1.133(3), N2−C3 1.470(4), C3−C4 1.517(4), C3−C5 1.512(4), C3−C6 1.507(5); C1−B−C11 104.5(2), C1−B−C21 103.1(2), C1−B−C31 107.6(2), C11−B−C21 114.6(2), C11−B−C31 114.4(2), C21−B−C31 111.5(2), B−C1−N2 174.7(3), C1−N2−C3 173.1(3), N2−C3−C4 105.1(3), N2−C3−C5 107.3(3), N2−C3−C6 107.4(3), C4−C3−C5 112.4(3), C4−C3−C6 112.4(3), C5−C3−C6 11.7(3).

tetrahedral coordination geometry around boron as revealed by the X-ray crystal structure analysis of **3a**. The average C(aryl)−B−C(aryl) angle amounts to 113.5(2)°; the average C1−B−C(aryl) angle is 105.1(2)° (see Figure 3). As expected, the isonitrile−boron moiety is linear (angle N2−C1−B 174.7(3)°), with both the carbon atom C1 and the nitrogen center N2 probably being sp-hybridized (angle C1−N2−B 173.1(3)°). The newly formed B−C1 linkage has a bond length of 1.624(4) Å, which is slightly below the typical B−C(sp^2) bond lengths of the adjacent B−C(aryl) linkages (average value 1.633(4) Å). The N≡C bond length of the coordinated isonitrile ligand in compound **3a** is 1.133(3) Å (i.e. C1−N2), which is ca. 1% *shorter* than the typical −N≡C triple bond length of the uncoordinated aliphatic isonitrile (1.145(5) Å).[28] Although this reduction of the N≡C bond length in **3a** may seem small, it is clearly noticeable and it represents a larger effect than observed upon *tert*-butylisonitrile coordination to the

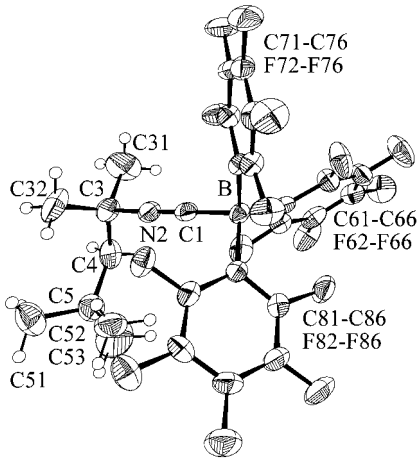

Figure 4. Molecular structure of **3b**. Selected bond lengths (Å) and angles (deg): B−C1 1.624(4), B−C61 1.637(4), B−C71 1.639(4), B−C81 1.624(4), C1−N2 1.136(3), N2−C3 1.473(4), C3−C4 1.536(4), C4−C5 1.534(4); C1−B−C61 106.2 (2), C1−B−C71 105.1(2), C1−B−C81 105.1(2), C61−B−C71 111.6(2), C61−B−C81 113.9(2), C71−B−C81 114.0(2), B−C1−N2 177.9(3), C1−N2−C3 172.7(3), N2−C3−C4 107.0(2), C3−C4−C5 123.5(3).

charged d^0-Lewis acid Cp$_3$Zr$^+$: free Me$_3$C−N≡C and the [Me$_3$C−N≡C−ZrCp$_3$]$^+$ complex **4a** exhibit identical $d_{C\equiv N}$ values within the experimental accuracy.[29] Coordination of Me$_3$C−N≡C to the charged Cp$_3$M$^+$ systems leads to a noticeable shift of the IR $\tilde{\nu}_{C\equiv N}$ band to higher wavenumbers (free Me$_3$C−N≡C $\tilde{\nu}$ = 2140 cm^{-1}; Zr-complex **4a**[29] 2209 cm^{-1}; Hf-complex **4b**[30] 2211 cm^{-1}; Me$_3$C−N≡C−BMe$_3$[31] **5** 2247 cm^{-1}). The corresponding IR effect upon binding Me$_3$C−N≡C to B(C$_6$F$_5$)$_3$ is much larger, as was to be expected from the observed crystallographic bond-shortening effect. The corresponding isonitrile band in the Me$_3$C−N≡C−B(C$_6$F$_5$)$_3$ addition product **3a** was found shifted to $\tilde{\nu}_{C\equiv N}$ = 2310 cm^{-1}.

We have prepared two additional R−N≡C/B(C$_6$F$_5$)$_3$ adducts. The 2,6-dimethylphenylisocyanide/tris(pentafluorophenyl)borane adduct **3c** was characterized by elemental analysis and spectroscopically. Again, a substantial IR $\tilde{\nu}_{C\equiv N}$ increase was observed (Δ = +53 cm^{-1}, $\tilde{\nu}$(C≡N) of **3c** 2275 cm^{-1}). The $\Delta\tilde{\nu}$(free RN≡C/coordinated RN≡C) value of the Me$_3$C−CH$_2$CMe$_2$−N≡C/B(C$_6$F$_5$)$_3$ **3b** addition product is even larger at ca. +170 cm^{-1} ($\tilde{\nu}_{C\equiv N}$ of **3b** 2301 cm^{-1}). Compound **3b** was also characterized by an X-ray crystal structure analysis. The essential structural parameters are very similar to those of **3a** (see Figure 4). The isonitrile-C≡N bond length also is slightly *decreased* upon coordinating Me$_3$C−CH$_2$CMe$_2$−N≡C/B(C$_6$F$_5$)$_3$ (d(C1−N2) = 1.136(3) Å found for **3b**), which shows that the observed structural and spectroscopic trend in the series of compounds investigated in this study appears experimentally consistent.

Finally, the Ph$_3$P−B(C$_6$F$_5$)$_3$ addition product **6**, which had already been prepared by Stone et al. early on, was also characterized by X-ray diffraction for comparison. For details see Figure 5 and the Experimental Section.

(28) Allen, F. H.; Kennard, O.; Watson, D. G.; Brammer, L.; Orpen, A. G.; Taylor, R. *J. Chem. Soc., Perkin Trans.* **1987**, *2*, S1.

(29) Brackemeyer, T.; Erker, G.; Fröhlich, R. *Organometallics* **1997**, *16*, 531.

(30) Jacobsen, H.; Berke, H.; Brackemeyer, T.; Eisenblätter, T.; Erker, G.; Fröhlich, R.; Meyer, O.; Bergander, K. *Helv. Chim. Acta* **1998**, *81*, 1692.

(31) Casanova, J.; Schuster, R. E. *Tetrahedron Lett.* **1964**, 405.

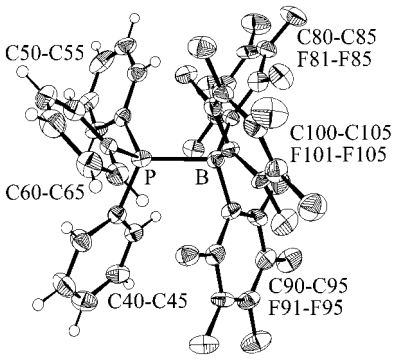

Figure 5. Molecular structure of $Ph_3P-B(C_6F_5)_3$ **6**. Selected bond lengths (Å) and angles (deg): P−B 2.180(6), B−C80 1.633(7), B−C90 1.636(7), B−C100 1.639(7), P−C40 1.831(5), P−C50 1.818(5), P−C60 1.821(5); P−B−C80 105.5(3), P−B−C90 105.4(3), P−B−C100 105.0(3), C80−B−C90 112.8(4), C80−B−C100 112.6(4), C90−B−C100 114.5(4), B−P−C40 113.5(2), B−P−C50 113.3(2), B−P−C60 114.1(2), C40−P−C50 105.3(2), C40−P−C60 104.2-(2), C50−P−C60 105.4(2).

We conclude that the examples experimentally investigated in the course of this study show that coordination of the nitriles as well as the isonitriles to the neutral Lewis acid tris(pentafluorophenyl)borane leads to a substantial increase in the C≡N bond strength. This is evident from a marked shift of the $\tilde{\nu}_{C\equiv N}$ IR band to higher wavenumbers, and this interpretation is supported by the observed small but experimentally significant decrease of the C≡N bond length observed by X-ray diffraction. Both these effects are markedly stronger for coordination of the nitriles and isonitriles to the neutral $B(C_6F_5)_3$ Lewis acid than to the positively charged organometallic d_0-Cp_3M^+ system (M = Zr, Hf). Electrostatic effects have quite convincingly been shown to be dominant in the latter charged systems and must probably be held responsible for the bond-strengthening effect in the $[Cp_3Zr-C\equiv NR]^+$ (**4**) and $[Cp_3Zr-N\equiv CR]^+$ (**2**) systems. The question remains whether electrostatic features are similarly effective in causing the analogous but even more pronounced bond-strengthening effects in the neutral adduct systems **1** and **3**, respectively, or if other reasons should be considered in these cases. A detailed theoretical analysis has been carried out to provide a reasonable answer to this problem.

Theoretical Studies. Bonding Analysis. Help to answer the question as posed above is provided by an energy decomposition scheme, which we use in our bonding analysis.[32] We will thus begin the theoretical discussion with a concise description of this particular procedure. We will examine the B−L bond energy in R_3B-L complexes by examining the bond-forming reaction between the Lewis acid and the Lewis base fragments:

$$R_3B + L \rightarrow R_3B-L \qquad (1)$$

The energy associated with reaction 1 is called the bond snapping energy BE_{snap}. It can be broken down into three main components, namely the electrostatic interaction, ΔE_{elstat}, the Pauli repulsion, ΔE_{Pauli}, and the orbital interaction term, ΔE_{int}:

$$BE_{snap} = -[\Delta E_{elstat} + \Delta E_{Pauli} + \Delta E_{int}] \qquad (2)$$

Since electrostatic effects will play a major role in our discussion, we will describe the first term of eq 2 in more detail. ΔE_{elstat} describes the classical Coulomb interaction between the unmodified and interpenetrating charge distributions of fragments A and B:[33]

$$\Delta E_{elstat} = \frac{Z_A Z_B}{R} + \int \frac{\rho_A(1)\,\rho_B(2)}{|r_1 - r_2|}\,dr_1\,dr_2 + \int \rho_A(1) V_N^B\,dr_1 + \int \rho_B(1) V_N^A\,dr_1 \qquad (3)$$

In eq 3, the first two terms are the repulsive nucleus−nucleus and electron−electron interactions, while the last two terms are attractive interactions between the electron density on one nucleus and the positive point charge of the other nucleus. ΔE_{elstat} is in general attractive, since the second term decreases when A and B start to overlap, leading to a dominance of the electron−nucleus interaction terms.

ΔE_{Pauli} in eq 2 is termed exchange repulsion or Pauli repulsion and takes into account the destabilizing two-orbital four-electron interactions between occupied orbitals on both fragments. ΔE_{elstat} and ΔE_{Pauli} are often combined to yield the steric interaction term $\Delta E°$, but here we will deal with these contributions separately.

The last term in eq 2, ΔE_{int}, introduces the attractive orbital interaction between occupied and virtual orbitals on the two fragments and includes polarization and charge-transfer contributions.

To emphasize the importance of ΔE_{elstat} for chemical bonding, one might combine ΔE_{Pauli} and ΔE_{int} into the orbital term ΔE^{orb}:

$$\Delta E^{orb} = \Delta E_{Pauli} + \Delta E_{int} \qquad (4)$$

This definition can be justified if we keep in mind that both terms on the right side of eq 4 basically stem from interactions between orbitals on fragments A and B; the repulsive interaction between occupied orbitals on both fragments gives rise to ΔE_{Pauli}, and the attractive interaction between occupied orbitals on one center and virtual ones on the other originates in ΔE_{int}. For the bond snapping energy we now have

$$BE_{snap} = -[\Delta E_{elstat} + \Delta E^{orb}] \qquad (5)$$

Since the equilibrium geometry of the fragments usually differs from their arrangement in the final molecule, a geometric preparation energy ΔE_{prep} is needed to get the fragments ready for bonding. For R_3B-L systems, this is mainly the energy required to distort the BR_3 units from the planar ground state to the pyramidal fragment geometry. The bond energy BE then writes as

$$BE = BE_{snap} - \Delta E_{prep} \qquad (6)$$

(32) (a) Ziegler, T.; Rauk, A. *Theor. Chim. Acta* **1977**, *46*, 1. (b) Ziegler, T. Rauk, A. *Inorg. Chem.* **1979**, *18*, 1558. (c) Ziegler, T. *NATO ASI* **1992**, *C378*, 367. (d) Bickelhaupt, F. M.; Nibbering, N. M. M.; van Wezenbeek, E. M.; Baerends, E. J. *J. Phys. Chem.* **1992**, *96*, 4864.

(33) van den Hoeck, P. J.; Kleyn, A. W.; Baerends, E. J. *Comments At. Mol. Phys.* **1989**, *23*, 93.

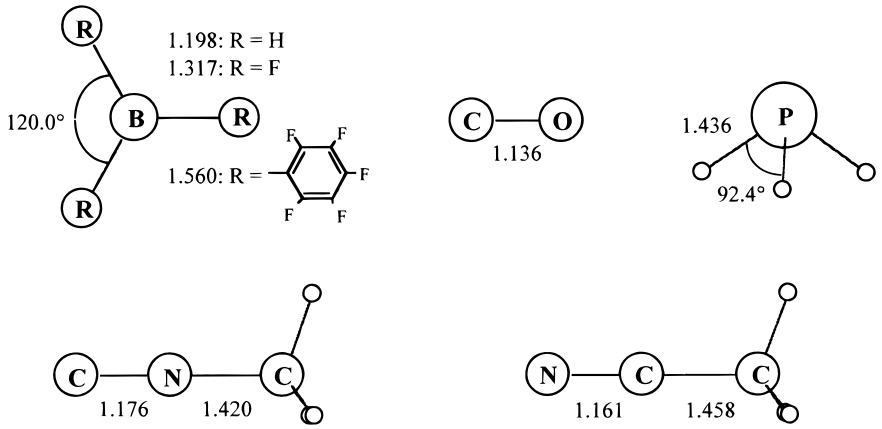

Figure 6. Optimized bond distances (in Å) and bond angles for the ground-state geometries of the fragment molecules.

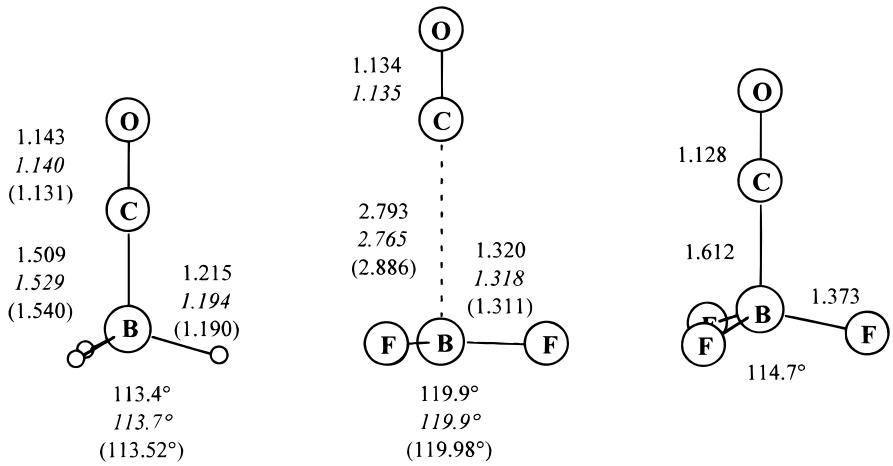

Figure 7. Optimized DFT-BP86 geometries (distances in Å) for $H_3B{\cdot}CO$, $F_3B{\cdot}CO$, and $F_3B{\cdot}CO$ with fixed B−C bond distances. Comparison with Bauschlicher and Ricca's DFT-B3LYP calculation (italics, ref 6) and experimental values (in parentheses, ref 4b ($H_3B{\cdot}CO$) and ref 7 ($F_3B{\cdot}CO$)).

If the bond energy is corrected for the difference in zero-point energy of the final molecule and the constituting fragments, we obtain the bond dissociation enthalpy at 0 K, $D°$:

$$D° = \mathrm{BE} - \Delta E_{\mathrm{ZPE}} \qquad (7)$$

The geometric changes of the fragments under bond formation will be of importance not only for bond energetics but also for bond analysis. Therefore, we present the optimized geometries of our fragment molecules in Figure 6. For important structural parameters, references to experimental data can be found in the following sections. For further information, we refer the reader to the recent literature.[6]

Structure and Bonding of $H_3B{\cdot}CO$ and $F_3B{\cdot}CO$. Since $H_3B{\cdot}CO$ has received considerable attention in the literature, we will refrain from a detailed discussion of all the features of this molecule. We will present only a concise comparison of the bonding characteristics of $H_3B{\cdot}CO$ and $F_3B{\cdot}CO$, to judge the performance of our theoretical approach, and to set the stage for a discussion of tris(pentafluorophenyl)borane donor complexes.

Optimized geometries for $R_3B{\cdot}CO$ complexes are displayed in Figure 7.

Our values conform with the DFT-B3LYP results of Bauschlicher and Ricca, and both calculations do agree well with the experiment, at least as far as the geometry of the BR_3 fragment is concerned. The calculations do represent the fact that $F_3B{\cdot}CO$ possesses an unusually long B−C bond distance, which is however underestimated by roughly 0.1 Å. This discrepancy has been reasoned before; [6] since the potential well for the B−C bond stretch is extremely shallow, small errors in well depth already result in a sizable error in the geometry.

Of further interest is the geometry of the CO ligand. For the donor complex with BH_3 we find that d_{CO} elongates by about 0.01 Å. The experimental bond distance is essentially the same as in the free ligand[34] (d_{CO} = 1.128 Å). For the complex with BF_3, it can be seen that both the CO and BF_3 undergo only insignificant changes in geometry when forming the van der Waals complex.

Information about chemical bonding can be provided by an analysis of the stretching frequencies. Of particular interest are the CO as well as the B−C stretching modes, for which the wavenumbers are compiled in Table 1.

Our calculations indicate that for $H_3B{\cdot}CO$ the wavenumber for the CO stretch is almost identical to that of free CO, whereas in the experiment a shift to higher wavenumbers by 25 cm^{-1} can be observed. Furthermore, the B−C stretching mode is overestimated by about 87

(34) Huber, K.-P.; Herzberg, G. *Molecular Spectra and Molecular Structure.* Vol IV. *Constants of Diatomic Molecules*; Van Nostrand Reinhold: New York, 1979.

Table 1. Selected Stretching Wavenumbers[a] for $H_3B{\cdot}CO$ and $F_3B{\cdot}CO$

	$\tilde{\nu}_{C\equiv O}$			$\tilde{\nu}_{B-C}$		
	this work	BR[b]	exp	this work	BR[b]	exp
CO	2126	2211	2143[c] 2138.7[d]			
$H_3B{\cdot}CO$	2125	2219	2164.7[e]	778	753	691.4[e]
$F_3B{\cdot}CO$	2147	2236	2150.7[d]	73	86	65(8)[f]

[a] In cm^{-1}. [b] Ref 6. [c] Ref 34. [d] Ref 35. Obtained in Ar-matrix at $T = 15-30$ K. [d] Ref 4f. [f] Ref 7.

Table 2. Bond Dissociation Energies[a] $D°$ for $R_3B{\cdot}CO$ Complexes, R = H, F

	BE	ΔE_{ZPE}	$D°$	$D°$ (BR)[b]	$D°$(expt)
$H_3B{\cdot}CO$	155	13	142	114	141[c] 92[d] 97 ± 8[e] ≤ 99[f] 79[g]
$F_3B{\cdot}CO$	5	2	3	11	7.6 ± 0.3[h]

[a] In kJ/mol. If necessary, literature values have been transformed and rounded. [b] Ref 6. DFT-B3LYP. [c] Ref 4k. [d] Ref 4i. [e] Ref 4h. [f] Ref 4 g. [g] Ref 4e. [h] Ref 9.

cm^{-1}. The results for $F_3B{\cdot}CO$ show better agreement with the experiment. The observed shift to higher wavenumbers for $\tilde{\nu}_{C\equiv O}$ is well reproduced, and the B−C stretching mode at very low energy also closely matches the result from a microwave study.[35] Bauschlicher and Ricca's CO stretches show better qualitative agreement with the experimental trends, although in absolute terms the BP86 calculation is closer to the measured values.

Goldmann and Krogh-Jespersen[18,36] have thoroughly analyzed the origin of the increase in the C≡O stretching force constant F_{CO}, which corresponds to an increase in $\tilde{\nu}_{C\equiv O}$ and a decrease in the C≡O bond length upon coordination of carbon monoxide to cationic species. They conclude that electrostatic effects rather than donation from the 5σ orbital of CO are responsible for these effects. Although σ donation is an important factor in the bonding of CO to transition metal centers, Goldmann and Krogh-Jespersen found that F_{CO} values can be quantitatively interpreted by using a model only invoking M−CO π back-bonding and an electrostatic parameter. In connection with this problem, they also discuss the $H_3B{\cdot}CO$ molecule, and we refer the reader back to their work[18] for further details.

In what follows, we try to adapt some of the qualitative concepts connected with the examination carried out by Goldmann and Krogh-Jespersen. At the onset, we note that from our frequency analysis we might conclude that the calculated B−C bond strength is probably too high (compare $\tilde{\nu}_{B-C}$, experimental and theoretical values) and that the reason for this is an overestimation of π back-bonding, since an increase in π bonding will strengthen the B−C bond, but will also cancel the effect of increasing $\tilde{\nu}_{C\equiv O}$ due to electrostatic effects.

In Table 2, computed dissociation energies and experimental data are presented.

Although our calculated value for $H_3B{\cdot}CO$ lies within the range of experimentally established values, it is more likely that the true bond dissociation energy lies around 90 kJ/mol. This is supported by the very accurate coupled cluster calculations on the CCSD(T) level by Bauschlicher and Rica, which yield for the bond dissociation energy of $H_3B{\cdot}CO$ a value of 88 kJ/mol.[6] It seems that DFT calculations indeed overestimate the $H_3B{\cdot}CO$ bond energy; this effect is somewhat stronger at the BP86 than at the B3LYP level. For $F_3B{\cdot}CO$, the DFT calculations verify the experimental finding of a very weak B−C linkage, on the order of magnitude of a few kJ/mol.

We will now turn to the bond analysis, according to eq 2. Besides the scheme presented here, there exist several others in the literature, and $H_3B{\cdot}CO$ has been subjected to the KM (Kitaura−Morokuma),[5a,37] NEDA (natural energy decomposition analysis),[5e] and CSOV (constrained-space-orbital variation)[6,38] approaches; the latter was also applied to $F_3B{\cdot}CO$. Since this molecule is only weakly bound, as discussed before, we perform the analysis with a fixed distance d_{C-B} that corresponds to the calculated values for the hypothetical complex $(C_6F_5)_3B{\cdot}CO$ (vide supra). The results of this analysis are summarized in Table 3, and the conclusions reached are similar to those obtained from other bond analysis schemes. Characteristic features for the BF_3 complex in comparison with its BH_3 analogue are an increase in electrostatic binding, a weaker orbital interaction, and a stronger Pauli repulsion. The analysis for $F_3B{\cdot}CO$ is somewhat arbitrary, since it is not performed for the equilibrium geometry. The general trends, however, become clear. It should be noted that in terms of BE_{snap} both molecules $H_3B{\cdot}CO$ and $F_3B{\cdot}CO$ are energetically stable. It is the contribution of the preparation energy ΔE_{prep} that renders a geometry with a short B−C contact unstable in the case of $F_3B{\cdot}CO$.

The nature of the electronic interaction energies might be analyzed in terms of a Mulliken fragment population analysis. The total population of the formerly empty virtual orbitals of the BR_3 fragment in the final molecule serves as a measure for σ donation, whereas the electron donation to the virtual orbitals of the CO molecule indicates the amount of π back-donation. BH_3 and BF_3 are comparably good electron acceptors; the somewhat higher value for σ donation in the case of BH_3 is explained by the shorter B−C bond distance. Our analysis reveals that in the case of BH_3 there is also π back-bonding to the CO moiety, which stems from a combination of ligand-based orbitals having the appropriate symmetry properties. This effect induces an elongation of the CO bond length, which counteracts the electrostatic CO bond contraction. Overall, the calculated CO bond length in $H_3B{\cdot}CO$ appears to be slightly elongated. In comparison with the experimental results, it seems that it is this particular contribution to ΔE_{int}, namely the π back-donation, that is overestimated in the DFT calculations, as previously concluded. The back-bonding in $F_3B{\cdot}CO$ is present, but less pronounced than that for $H_3B{\cdot}CO$. The σ/π ratio for the first amounts to 3.6, compared to 1.3 for the second. Conse-

(35) Gebicki, J.; Liang, J. *J. Mol. Struct.* **1984**, *117*, 283.
(36) A study similar to that of ref 18 was presented by Frenking and co-workers: Lupinetti, A. J.; Fau, S.; Frenking, G.; Strauss, S. H. *J. Chem. Phys.* **1997**, *101*, 9551.
(37) Kitaura, K.; Morokuma, K. *Int. J. Quantum Chem.* **1976**, *10*, 325.
(38) Bagus, P. W.; Hermann, K.; Bauschlicher, C. W., Jr. *J. Chem. Phys.* **1984**, *80*, 4378.

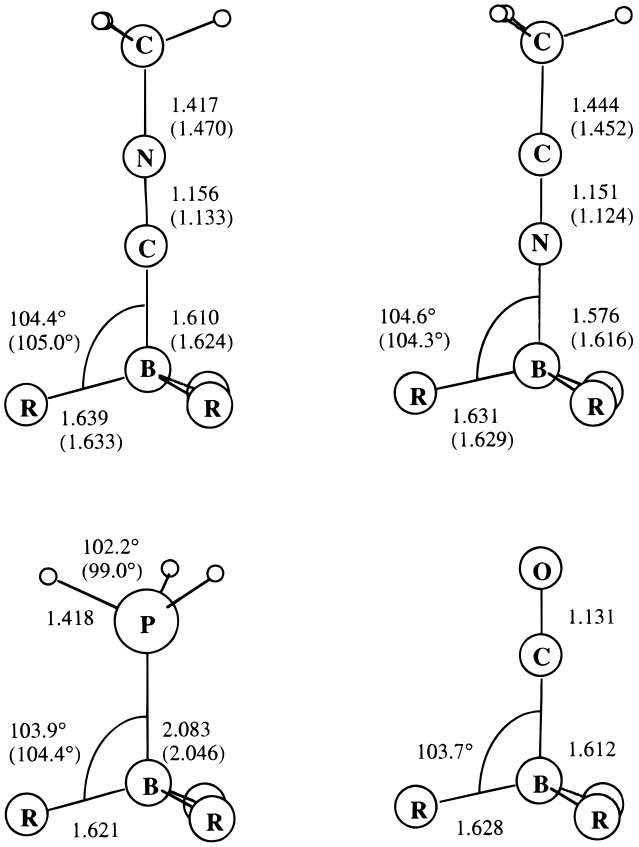

Figure 8. Selected geometric parameters (averged values, distances in Å) for various $(C_6F_5)_3B{\cdot}L$ complexes from DFT calculations and X-ray structure analysis (in parentheses). For the isonitrile complex, the experimental values refer to $(C_6F_5)_3B{\cdot}NC{-}C(CH_3)_3$.

quently, the electrostatic contraction dominates, and we find a shortened CO bond for the hypothetical $F_3B{\cdot}CO$ geometry. We wish to reiterate that dominance of the electrostatic terms in the bond energy over contributions due to π back-bonding causes contraction of the CO bond length in accordance with a shift of the $\tilde{\nu}_{CO}$ stretch to higher wavenumbers.

This in turn leads us to question how tris(pentafluorophenyl)borane, $B(C_6F_5)_3$, might interact with CO. Intuitively, we would expect that $B(C_6F_5)_3$ would undergo strong electrostatic interactions comparable to or even higher than those of BF_3. On the other hand, we would also anticipate a stronger orbital interaction due to an enhanced π component, since the C-based orbitals responsible for donation in $B(C_6F_5)_3$ are higher in energy than their F-based counterparts in BF_3 and do provide a better energetic match with the accepting π orbitals of the CO group. Before we analyze the $B(C_6F_5)_3$ bonding with prototypical donor−acceptor ligands in detail, we will begin the next section with a discussion of the optimized molecular geometries when compared with experimental results obtained from X-ray structure analysis.

Structures of Donor Complexes of Tris(pentafluorophenyl)borane. The calculated structures of $(C_6F_5)_3B{\cdot}L$ complexes, L = $CNCR_3$, $NCCH_3$, PH_3, CO, together with data from crystal diffraction are displayed in Figure 8.

The most interesting structural parameters are the B−L bond distances, as well as the C≡X triple bond lengths for the isonitrile, nitrile, and carbonyl complexes. We will limit our discussion to these two parameters, which offer some insight into the chemical bonding in these complexes. It should further be mentioned that in all cases the agreement between the calculated and measured structures of the $B(C_6F_5)_3$ units is high, with deviations of about 0.01 Å and 1° for bond lengths and bond angles, respectively.

For the isonitrile complex, the calculation slightly underestimates the B−L bond distance by about 0.01 Å, whereas for the boron nitrile adduct the computed distance d_{BN} falls short by 0.04 Å compared to the experiment. The opposite effect is found for the phosphine complex, for which the calculation overestimates the B−P separation by roughly the same amount instead. One of the donor−acceptor bond characteristics of BF_3 is that the interatomic distances in the gas phase tend to be larger than those for the solid state. An intriguing example of this is the complex $F_3B{\cdot}NCCH_3$, which has a B−N bond length of 2.011 Å in the gas phase[39] and a 1.630 Å bond length in the solid state.[40] We might expect a similar but less pronounced effect in tris(pentafluorophenyl)borane complexes, and on the basis of these observations we could explain the longer B−P bond of the gas-phase calculation as compared to the solid-state structure. The fact that the gas-phase calculations for the isonitrile and nitrile complexes yield short B−L bonds might again indicate that our calculations overestimate the B−L bond strength in systems containing good π acceptor ligands. On coordination to the boron center, the angle ∠(HPH) opens up by roughly 10°; the same is found in the experiment, where the angle ∠(HPH) changes from 93.345° in the free ligand[41] to about 104° in the $(C_6F_5)_3B$ adduct. This indicates a rehybridization of the P-center, which adopts a quasi tetrahedral coordination. The same effect, although less pronounced, is observed in $(C_6F_5)_3B{\cdot}PPh_3$, where the angle changes from 102° for the free ligand[42] to 105° in the complex. Not only does the increased steric bulk of the phosphine ligand influence the cone angle but it also leads to a lengthening of the B−P bond, which in the case of $(C_6F_5)_3B{\cdot}PPh_3$ is about 0.1 Å longer than in phosphine. This highlights the fact that the potential energy surface around the B−L equilibrium distance is shallow, allowing for a large variation in the bond length, a characteristic feature of dative bonds when contrasted with covalent bonds.[43]

Both the experimental and the theoretical studies result in a shortening of the C≡X triple bond when $CNCR_3$, $NCCH_3$, or CO coordinates to $(C_6F_5)_3B$. These changes are compiled in Table 4.

The bond contraction $\Delta d_{C\equiv X}$ is compatible for experiment and theory and lies within 0.01−0.02 Å. The calculation suggests that the contraction should be larger for the isonitrile than for the nitrile, whereas the

(39) Dvorak, M. A.; Ford, R. S.; Suenram, R. D.; Lovas, F. J.; Leopold, K. R. *J. Am. Chem. Soc.* **1992**, *114*, 108.
(40) (a) Hoard, J. L.; Owen, T. B., Buzzell, A, Salmon, O. N. *Acta Crystallogr.* **1950**, *3*, 130. (b) Swanson, B.; Shriver, D. F.; Ivers, J. A. *Inorg. Chem.* **1969**, *8*, 2182.
(41) Helms, D. A.; Gordy, W. *J. Mol. Spectrosc.* **1977**, *66*, 206.
(42) (a) Daly, J. J. *J. Chem. Soc.* **1964**, 3799. (b) Dunne, B. J.; Orpen, A. G. *Acta Crystallogr.* **1991**, *47C*, 345. (c) Cheklov, A. N. *Kristallografiya* **1993**, *38*, 79. (d) Bruckmann, J.; Krüger, C.; Lutz, F. *Z. Naturforsch.* **1995**, *50B*, 351.
(43) Haaland, A. *Angew. Chem.* **1989**, *101*, 1017; *Angew. Chem., Int. Ed. Engl.* **1989**, *30*, 1160.

Table 3. Bond Analysis[a] and Mulliken Populations[b] by Virtual Fragment Orbitals for $R_3B{\cdot}CO$ Complexes, R = H, F

	ΔE_{elstat}	ΔE_{Pauli}	ΔE_{int}	BE_{snap}	ΔE_{prep}	BE	$\sigma(CO\rightarrow B)$[d]	$\pi(B\rightarrow CO)$[d]
$H_3B{\cdot}CO$	−310	635	−536	211	56	155	0.58	0.44
$F_3B{\cdot}CO$[c]	−327	670	−386	43	86	−43	0.50	0.14

[a] Energies in kJ/mol. [b] In au. [c] Geometry optimized with fixed B−C bond distance (see text). [d] B = H_3B or F_3B, respectively.

Table 4. Changes in the C≡X Bond Length of $CNCR_3$, $NCCH_3$, and CO under Coordination to $(C_6F_5)_3B$

	$d_{C\equiv X}$ experiment[a]			$d_{C\equiv X}$ theory[a]		
	free	coordinated	Δ	free	coordinated	Δ
$R_3B-CNCMe_3$	1.145[b]	1.133	0.012			
$R_3B-CNMe$				1.176	1.156	0.020
$R_3B-NCMe$	1.141[c]	1.124	0.017	1.161	1.151	0.010
R_3B-CO				1.136	1.131	0.005

[a] In Å. [b] Ref 28. [c] Ref 26.

Table 5. Bond Analysis[a] for Various $(C_6F_5)_3B{\cdot}L$ Complexes

	ΔE_{elstat}	ΔE_{Pauli}	ΔE_{int}	BE_{snap}	ΔE_{prep}	BE
$R_3B-CNMe$	−483	839	−562	206	94	112
$R_3B-NCMe$	−413	742	−483	154	90	64
R_3B-PH_3	−330	603	−419	146	94	52
R_3B-CO	−385	791	−519	113	75	38

[a] In kJ/mol.

experiment shows a somewhat larger contraction for acetonitrile compared to *tert*-butylisonitrile. The steric bulk of the *tert*-butyl group offers a possible explanation for this observation, as well as for the unusual long C−N bond when compared with the computed values (compare Figures 6 and 8). All this indicates that again electrostatic effects are of importance in the bonding of $(C_6F_5)_3B{\cdot}L$ complexes, which we will analyze in the next section.

Bonding of Donor Complexes of Tris(pentafluorophenyl)borane. The results of our bonding analysis according to eq 2 are collected in Table 5. We will first analyze the bonding for the three C≡X donors. The terms ΔE_{int}, ΔE_{Pauli} and ΔE_{elstat} are on the same order of magnitude partly with different signs and show similar differences, but only the last term parallels the observed order of coordination effects. It is thus the relative size of the electrostatic energy (CNMe > NCMe > CO) and not the orbital interaction energy (CNMe > CO > NCMe) that determines the ranking in the bond snapping energy (CNMe > NCMe > CO). Furthermore, the relative differences in ΔE_{elstat} for the different donors L are similar to those found for BE_{snap}. From this we might conclude that the bonding in $(C_6F_5)_3B{\cdot}L$ complexes indeed is dominated by electrostatic effects. The formation of all complexes requires the distortion of the planar $(C_6F_5)_3B$ molecule into its pyramidal fragment geometry, which leads to sizable contribution of the preparation energy, and leads to a weakening of the B−L by about 75−100 kJ/mol. Thus, the complex $(C_6F_5)_3B{\cdot}CO$ has a bond energy of only 38 kJ/mol and is rather weakly bound. If we apply the zero point energy correction, taking the $H_3B{\cdot}CO$ value as a first estimate, we arrive at a value of 25 kJ/mol for the bond dissociation enthalpy at 0 K. If we further take entropy terms into account—again obtained as estimates from $H_3B{\cdot}CO$—we get for the reaction $(C_6F_5)_3B + CO \rightarrow (C_6F_5)_3B{\cdot}CO$ a value of $\Delta G \approx 40$ kJ/mol at 298 K and $\Delta G \approx 0$ kJ/mol at 200 K in the gas phase. This suggests that the complex $(C_6F_5)_3B{\cdot}CO$ does not possess much thermodynamic stability. The crystal environment, however, might substantially stabilize the $(C_6F_5)_3B{\cdot}CO$ molecule (vide infra) and might allow for its isolation in the solid state.

The interaction between $(C_6F_5)_3B$ and CO also allows us to assess the bonding properties of this Lewis acid in comparison to the prototypes for the respectively soft and hard acids BH_3 and BF_3. As we anticipated earlier, the electrostatic component of the B−L bond even exceeds the value for BF_3 and BH_3 by roughly 70 kJ/mol. We also find that the term ΔE_{int} is comparable to that for BH_3 and significantly larger than that of BF_3. However, due to the extended size, and therefore to the extended electronic core, we also find an increase in Pauli repulsion so that $(C_6F_5)_3B$ ranks between BH_3 and BF_3 in terms of overall bonding energy.

A somewhat different situation is found for the phosphine ligand. We now have significant smaller bonding terms ΔE_{elstat} and ΔE_{int}, but also a smaller repulsion term ΔE_{Pauli}. This is a direct consequence of the much longer B−L bond distance. As a final result, the subtle balance between attractive and repulsive bond terms places the PH_3 ligand between $NCCH_3$ and CO in terms of the B−L bond strength (see Table 5).

The strength of the B−P bond in $(C_6F_5)_3B{\cdot}PH_3$ has been estimated in experimental studies. Crystals of this compound lose phosphine when heated in vacuo, and static vapor pressure measurements suggest an enthalpy of dissociation of about 80 kJ/mol.[14] This value is about one and a half times higher than the (uncorrected) computed value, which should decrease further when the zero-point energy correction is taken into account. A possible explanation for this may be that the crystal environment prevents a spontaneous relaxation of the $(C_6F_5)_3B$ into its equilibrium geometry. This would imply that for an estimate of BE(B−P) we only have to consider the preparation energy of PH_3. When doing so, we get for BE(B−P) a value of 129 kJ/mol. Applying zero-point energy and temperature correction, as estimated from a calculation on $H_3B{\cdot}PH_3$, we obtain for the enthalpy of bond dissociation at 298 K $\Delta H \approx 100$ kJ/mol, in fair agreement with the experimental value. Weak B−L bonds might thus be substantially stabilized in a crystal environment.

We conclude this section with a closer look at the orbital interaction term ΔE_{int}, and we will once more use a Mulliken fragment population analysis to assess the relative importance of σ donation vs π back-donation. Our results are compiled in Table 6. For C≡X ligands, the σ donation is about 5 times greater than the π back-donation and represents the dominant orbital interaction. This is in sharp contrast with the case of classical transition metal complexes, in which the π component is equal to, or more important than,

Table 6. Mulliken Fragment Population Analysis[a] for Various (C_6F_5)$_3$B·L Complexes

	σ(CO→B)[b]	π(B→CO)[b]	σ/π
$R_3B-CNMe$	0.66	0.14	4.71
$R_3B-NCMe$	0.53	0.10	5.30
R_3B-PH_3	0.60	0.16	3.75
R_3B-CO	0.58	0.22	2.64

[a] In au. [b] B = (C_6F_5)$_3$B.

the σ contribution.[19,44,45] Nevertheless, a π component is present, and its nature is similar to that of the one discussed for BH_3. In relation to the σ/π ratio, we would like to present another argument which corroborates our findings for electrostatic effects being responsible for C≡X bond shortening. One common argument used to explain a C−X distance decrease under complex formation is that of increased σ donation. The 5σ orbital in CO is assumed to possess some C−O antibonding character.[46] Hence, OC→B donation should remove electron density from this orbital and consequently strengthen and shorten the bond. On the other hand, π back-donation counteracts this effect. This would imply that the ligand showing the highest σ/π ratio should show the largest bond contraction $\Delta d_{C\equiv X}$. In contrast, our calculation show that $\Delta d_{C\equiv X}$ does not correlate with σ/π ratio, but rather with the ΔE_{elstat} size, in agreement with Goldmann and Krogh-Jespersen.[18] The experimental data obtained from crystal structures do not quite confirm this trend; but the change in the $\tilde{\nu}_{C\equiv X}$ might clarify the picture. For the nitrile adducts, we find for $\Delta\tilde{\nu}_{C\equiv N}$ values of about 100 cm^{-1}, whereas for the isonitriles, with the exception of **3c**, $\Delta\tilde{\nu}_{C\equiv N}$ increases to about 170 cm^{-1}. This observation reflects the theoretical trend found for ΔE_{elstat}.

Comparison with Cationic Transition Metal Systems. As we have noticed earlier, the effects of a shift of $\tilde{\nu}_{C\equiv N}$ to higher wavenumbers and a shortening of the $d_{C\equiv N}$ are markedly stronger for coordination of the nitriles and isonitriles to the neutral B(C_6F_5)$_3$ Lewis acid than to the positively charged organometallic d_0-Cp_3Zr^+ system. The bond analysis for the latter systems also brought to light the importance of electrostatic effects.[30] This points to a necessary comparison between the main group complexes R_3B·L and the transition metal complexes [R_3Zr·L]$^+$. The results of the bonding analysis according to orbital terms and electrostatic terms (eq 5) are presented in Figure 9.

It might be surprising that the ΔE_{elstat} component is higher for the boron than for the zirconium complexes, even though the latter ones carry a positive charge. This is caused by the longer Zr−L bond of about 2.30 Å, which enters the electrostatic term as 1/*r*. As anticipated in the experiment, an enhanced electrostatic component seems to be responsible for more pronounced $\Delta\tilde{\nu}_{C\equiv N}$ and $\Delta d_{C\equiv N}$. Furthermore, we have not only an increase in ΔE_{elstat} but an enhanced Pauli repulsion as well, which is the dominant contribution to ΔE^{orb}. It is remarkable that the trend and the magnitude of BE_{snap} are essentially the same for the [R_3Zr·L]$^+$ and for the R_3B·L complexes. The bonding characteristics of the main group and the transition metal compounds appear to be strikingly similar, but the variation in ΔE_{elstat} manifests itself in the trends as mentioned above.

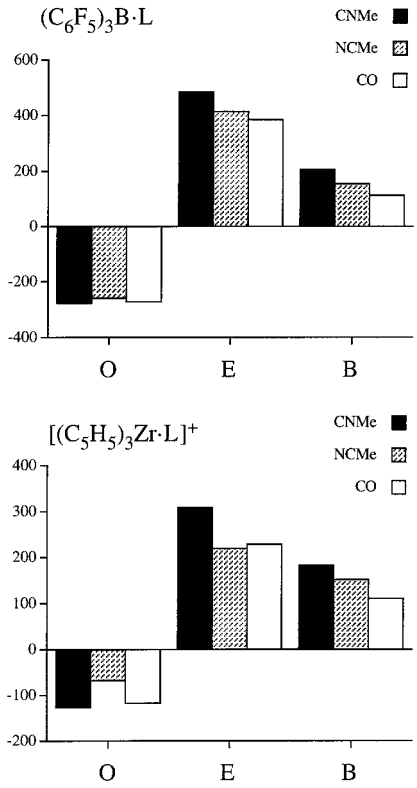

Figure 9. Energy decomposition (in kJ/mol) of the M−L bond for (C_6F_5)$_3$B·L and [Cp_3Zr·L]$^+$ complexes according to orbital terms and electrostatic terms. The negative of ΔE_{orb} and ΔE_{elstat} is shown, so that in any case positive energy values indicate stabilization, and vice versa. O stands for ΔE_{orb}, E for ΔE_{elstat}, and B for the bond snapping energy BE_{snap}.

The difference in Zr−L and B−L bonding is contributed by the preparation energy. The [Cp_3Zr]$^+$ fragment does not significantly change its geometry under coordination of the Lewis base. The acceptor orbital is an empty, metal-based d_{z^2} orbital, and rehybridization is not required as it is in the R_3B case. Thus, BE_{snap} is a good approximation of the bond energy BE. The Zr−L bonds are about 75−100 kJ/mol more stable than B−L linkages, and the transition metal complex is more likely to be formed.

Conclusion

We have prepared and characterized a series of donor adducts of tris(pentafluorophenyl)borane. For the nitrile and isonitrile complexes, it was found that $d_{C\equiv N}$ shortens and that $\tilde{\nu}_{C\equiv N}$ is shifted to higher wavenumbers under adduct formation. A theoretical analysis revealed that the bonding in (C_6F_5)$_3$B·L complexes is mainly dominated by electrostatic interactions, which in turn are responsible for the observed structural and spectroscopic changes.[19] In this respect, B(C_6F_5)$_3$ is similar to the hard Lewis acid BF_3, but an enhanced orbital interaction provides additional bond stabilization. In contrast to BF_3, the complex with carbon monoxide possesses some intrinsic thermodynamic stability and might be further stabilized by a crystal environment.

(44) Kraatz, H.-B.; Jacobsen, H.; Ziegler, T.; Boorman, P. M. *Organometallics* **1993**, *12*, 76.
(45) (a) Li, J.; Schreckenbach, G.; Ziegler, T. *J. Am. Chem. Soc.* **1995**, *117*, 486. (b) Ziegler, T.; Tschinke, V.; Ursenbach, C. *J. Am. Chem. Soc.* **1987**, *109*, 4825.
(46) Albright, T. A.; Burdett, J. K.; Whangboo, M.-H. *Orbital Interactions in Chemistry*; John Wiley: New York, 1985; p 78.

The bonding characteristics of $(C_6F_5)_3B{\cdot}L$ complexes are very similar to that of $[R_3Zr{\cdot}L]^+$, and the hypothetical $(C_6F_5)_3B{\cdot}CO$ can indeed be looked at as the main group analogue of a (nonclassical) transition metal carbonyl complex.

Computational Procedure

All calculations are based on the local density approximation (LDA) in the parametrization of Vosko, Wilk, and Nussair,[47] with the addition of gradient corrections due to Becke[48] and Perdew[49] (BP86), which were included self-consistently (NL-SCF). The calculations utilized the Amsterdam Density Functional package ADF,[50] release 2.3. Use was made of the frozen core approximation. For all elements, except for H and for the atoms of the pentafluorophenyl group, the valence shells were described using a triple ζ-STO basis, augmented by one d and one f STO polarization function (ADF database V). H was treated with a triple-ζ STO basis and one additional p and d STO polarization function (ADF database V), whereas for the members of the C_6F_5 moiety a double-ζ STO basis with one d polarization function was employed. For systems containing the BH_3 or BF_3 unit, calculations were performed in C_{3v} symmetry, the accuracy parameter for the numerical integration[50b] was chosen as 6.0, and final gradients in the geometry optimization were less than 2.5×10^{-4} au/Å. For $B(C_6F_5)_3$ systems, no symmetry constraints were employed, the numerical accuracy was set to 4.5, and final gradients were 2.5×10^{-3} au/Å and better. Default settings[51] were used for frequency calculations. The computations were carried out on DEC AlphaStations 500.

Experimental Section

General. All reactions were carried out under an argon atmosphere using Schlenk-type glassware or in a glovebox. Solvents (including deuterated solvents used for NMR spectroscopy) were dried and distilled under argon prior to use. The materials either were commercial products [acetonitrile, *p*-methylbenzonitrile, *p*-nitrobenzonitrile, *tert*-butylisocyanide, 1,1,3,3-tetramethylbutylisocyanide, 2,6-dimethylphenylisocyanide, triphenylphoshine] or were prepared following literature procedures [tris(pentafluorophenyl)borane].[20]

The following instruments were used for spectroscopic and physical characterization of the compounds: Bruker AC 200P and Bruker ARX 300 NMR spectrometers. Chemical shifts are referred to Me_4Si [δ^1H (C_6D_5H) = 7.15, δ^{13}C (C_6D_6) = 128.0], neat $BF_3{*}OEt_2$ [δ^{11}B = 0 for $\Xi(^{11}B)$ = 32.084 MHz], neat $MeNO_2$ [δ^{14}N = 0 for $\Xi(^{14}N)$ = 7.224 MHz, δ^{15}N = 0 for $\Xi(^{15}N)$ = 10.133 MHz], $CFCl_3$ [δ^{19}F = 0 for $\Xi(^{19}F)$ = 94.077 MHz], 80% H_3PO_4 in D_2O [δ^{31}P = 0 for $\Xi(^{31}P)$ = 40.4807 MHz]; Nicolet 5 DXC FT-IR spectrometer; melting points, DSC 2910 (Thermo Analysis/Du Pont); elemental analyses, Foss-Heraeus CHN-Rapid; X-ray crystal structure analyses, Enraf-Nonius CAD4 and MACH3 diffractometers (programs used: data reduction MolEN, structure solution SHELXS-86, structure refinement SHELXL-93, graphics SCHAKAL-92). Crystals of **1a**, **3a**, **3b**, and **6** were obtained from benzene solution by the diffusion method (pentane diffusion from the gas phase). Single crystals of **1c** were obtained from benzene-d_6.

General Procedure for the Preparation of the Complexes 1a, 1b, 3a, 3b, and 3c. To a solution of tris(pentafluorophenyl)borane in 100 mL of pentane was added dropwise a solution of the Lewis base (ca. 10% excess) in the same volume of pentane. The product began to precipitate immediately. After further stirring for 2 h at room temperature, the solid product was isolated by filtration, washed twice with 20 mL of pentane, and dried in vacuo. The products were obtained as colorless powders.

Tris(pentafluorophenyl)borane−Acetonitrile, Complex 1a. Tris(pentafluorophenyl)borane (1.00 g, 1.95 mmol) and 90 mg (2.19 mmol) of acetonitrile give the product **1a**. Yield of **1a**: 1.02 g (94%), mp 219 °C (DSC). $C_{20}H_3BF_{15}N$ (553.0): calcd C 43.43, H 0.55, N 2.53; found C 42.67, H 0.83, N 2.00. ^{1}H NMR (200.1 MHz, benzene-d_6): δ = 0.32 (s, 3H, CH_3). ^{13}C NMR (50.3 MHz, benzene-d_6): δ = 148.5 (dm, $^1J_{CF}$ = 246 Hz, $B(C_6F_5)_3$ (o-*C*)), 141.0 (dm, $^1J_{CF}$ = 252 Hz, $B(C_6F_5)_3$ (p-*C*)), 137.8 (dm, $^1J_{CF}$ = 254 Hz, $B(C_6F_5)_3$ (m-*C*)), −0.89 (*C*H_3), not observed *C*≡N and $B(C_6F_5)_3$ (ipso-*C*). ^{11}B NMR (64.2 MHz, benzene-d_6): δ = −10.3 ($\nu_{1/2}$ = 330 ± 10 Hz). ^{19}F NMR (282.4 MHz, benzene-d_6): δ = −134.7 (m, 2F, (m-*F*)), −154.8 (broad, 1F, (p-*F*)), −163.2 (m, 2F, (o-*F*)). IR (KBr): $\tilde{\nu}$ = 2367 (C≡N) cm^{-1}. X-ray crystal structure analysis of **1a**: formula $C_{20}H_3NBF_{15}$, M = 553.04, colorless, 0.40 × 0.20 × 0.10 mm, a = 10.944(1) Å, b = 9.288(1) Å, c = 19.384(1) Å, β = 90.39(1)°, V = 1970.3(4) Å^3, ρ_{calc} = 1.864 g cm^{-3}, μ = 2.09 cm^{-1}, empirical absorption correction via ψ scan data (0.983 ≤ C ≤ 0.998), Z = 4, monoclinic, space group $P2_1/n$ (No. 14), λ = 0.710 73 Å, T = 223 K, $\omega/2\theta$ scans, 7993 reflections collected (±h, +k, ±l), [(sin θ)/λ] = 0.62 Å^{-1}, 4001 independent and 2017 observed reflections [$I \geq 2\sigma(I)$], 335 refined parameters, R = 0.037, wR2 = 0.078, max. residual electron density 0.22 (−0.27) e·Å^{-3}, hydrogens calculated and riding.

Tris(pentafluorophenyl)borane−p-Methylbenzonitrile, Complex 1b. Tris(pentafluorophenyl)borane (1.00 g, 1.95 mmol) and 250 mg (2.13 mmol) of *p*-methylbenzonitrile give the product **1b**. Yield of **1b**: 1.13 g (92%), mp 180 °C (DSC). $C_{26}H_7BF_{15}N$ (629.1): calcd C 49.64, H 1.12, N 2.23; found C 49.22, H 1.47, N 2.28. ^{1}H NMR (200.1 MHz, benzene-d_6): δ = 6.90 (d, 2H, $^3J_{HH}$ = 8.11 Hz, Ph (m-*H*)), 6.38 (d, 2H, $^3J_{HH}$ = 8.11 Hz, Ph (o-*H*)), 1.68 (s, 3H, CH_3). ^{13}C NMR (50.3 MHz, benzene-d_6): δ = 148.7 (dm, $^1J_{CF}$ = 245 Hz, $B(C_6F_5)_3$ (o-*C*)), 143.4 (Ph (p-*C*)), 141.0 (dm, $^1J_{CF}$ = 252 Hz, $B(C_6F_5)_3$ (p-*C*)), 137.9 (dm, $^1J_{CF}$ = 254 Hz, $B(C_6F_5)_3$ (m-*C*)), 133.2 (Ph (o-*C*)), 130.6 (Ph (m-*C*)), 21.7 (*C*H_3); not observed *C*≡N, *C*-Me, Ph (ipso-*C*), and $B(C_6F_5)_3$ (ipso-*C*). ^{11}B NMR (64.2 MHz, benzene-d_6): δ = −9.6 ($\nu_{1/2}$ = 470 ± 10 Hz). ^{19}F NMR (282.4 MHz, benzene-d_6): δ = −134.7 (m, 2F, (m-*F*)), −155.6 (m, 1F, (p-*F*)), −163.2 (m, 2F, (o-*F*)). IR (KBr): $\tilde{\nu}$ = 2322 (C≡N) cm^{-1}.

Tris(pentafluorophenyl)borane−p-Nitrobenzonitrile, Complex 1c. Tris(pentafluorophenyl)borane (249 mg, 0.49 mmol) and 72 mg (0.49 mmol) of *p*-nitrobenzonitrile were mixed as solids, dissolved in 15 mL toluene, and stirred for 30 min at room temperature. After removing all volatile substances in vacuo 308 mg (0.47 mmol, 96%) of the pure product was obtained as a yellowish powder. Yield of **1c**: 0.308 g (96%), mp 183 °C (DSC). ^{1}H NMR (200.1 MHz, benzene-d_6): δ = 7.23 (m, 2H, AA′), 6.54 (m, 2H, BB′). ^{13}C NMR (50.3 MHz, benzene-d_6): δ = 151.3 (broad, *C*-NO_2), 148.6 (dm, $^1J_{CF}$ = 239 Hz, $B(C_6F_5)_3$ (o-*C*)), 141.2 (dm, $^1J_{CF}$ = 252 Hz, $B(C_6F_5)_3$ (p-*C*)), 137.8 (dm, $^1J_{CF}$ = 249 Hz, $B(C_6F_5)_3$ (m-*C*)), 133.8, 124.0 (Ph), 114.9, 113.2 (broad, =CCN/CN (without assignment)), 114.7 (broad, Ph (ipso-C)). ^{11}B NMR (64.2 MHz, benzene-d_6): δ = −10.2 ($\nu_{1/2}$ = 570 ± 10 Hz). ^{14}N NMR (14.5 MHz, benzene-d_6): δ = −11 ($\nu_{1/2}$ = 1550 ± 50 Hz). ^{19}F NMR (282.4 MHz, benzene-d_6): δ = −134.7 (broad, 2F, (m-*F*)), −154.8 (broad, 1F, (p-*F*)), −162.8 (broad, 2F, (o-*F*)). IR (KBr): $\tilde{\nu}$ = 2334 (C≡N) cm^{-1}. X-ray crystal structure analysis of **1c**: formula $C_{25}H_4N_2O_2BF_{15}$, M = 660.11, light yellow, 0.20 × 0.20 × 0.20 mm, a = 13.175(1) Å, b = 12.073(1) Å, c = 15.083(1) Å, β = 92.46(1)°, V = 2396.9(3) Å^3, ρ_{calc} = 1.829 g cm^{-3}, μ = 17.88 cm^{-1}, empirical

(47) Vosko, S. J.; Wilk, M.; Nussair, M. *Can. J. Phys.* **1980**, *58*, 1200.
(48) Becke, A. D. *Phys. Rev.* **1988**, *A38*, 3098.
(49) Perdew, J. P. *Phys. Rev.* **1986**, *B33*, 8822.
(50) (a) Baerends, E. J.; Ellis, D. E.; Ros, P. E. *Chem. Phys.* **1973**, *2*, 41. (b) teVelde, G.; Baerends, E. J. *J. Comput. Phys.* **1992**, *99*, 84. (c) Fonseca Guerra, C.; Visser, O.; Snijders, J. G.; te Velde, G.; Baerends E. J. In *Methods and Techniques in Computational Chemistry: METECC-95;* Clementi, E., Corongiu, G., Eds.; STEF: Cagliari, 1995; p 305.
(51) te Velde, G. *ADF 2.1 User's Guide*; Vrije Universiteit: Amsterdam, 1996.

absorption correction via ψ scan data ($0.949 \le C \le 0.998$), $Z = 4$, monoclinic, space group $P2_1/c$ (No. 14), $\lambda = 1.541\,78$ Å, $T = 223$ K, $\omega/2\theta$ scans, 9913 reflections collected ($\pm h, \pm k, -l$), [(sin θ)/λ] = 0.62 Å^{-1}, 4893 independent and 3725 observed reflections [$I \ge 2\sigma(I)$], 407 refined parameters, $R = 0.044$, wR2 = 0.124, max. residual electron density 0.25 (−0.19) e·Å^{-3}, hydrogens calculated and riding.

Tris(pentafluorophenyl)borane−tert-Butylisocyanide, Complex (3a). Tris(pentafluorophenyl)borane (1.00 g, 1.95 mmol) and 180 mg (2.17 mmol) of *tert*-butylisocyanide give the product **3a**. Yield of **3a**: 1.03 g (89%), mp 175 °C (DSC). $C_{23}H_9BF_{15}N$ (595.1): calcd C 46.42, H 1.52, N 2.35; found C 46.02, H 1.92, N 2.60. ^{1}H NMR (200.1 MHz, benzene-d_6): δ = 0.70 (s, 9H, (CH_3)$_3$C). ^{13}C NMR (50.3 MHz, benzene-d_6): δ = 148.6 (dm, $^1J_{CF}$ = 240 Hz, B(C$_6$F$_5$)$_3$ (o-*C*)), 140.8 (dm, $^1J_{CF}$ = 253 Hz, B(C$_6$F$_5$)$_3$ (p-*C*)), 137.7 (dm, $^1J_{CF}$ = 251 Hz, B(C$_6$F$_5$)$_3$ (m-*C*)), 80.7 ((CH$_3$)$_3$*C*−), 27.7 ((*C*H$_3$)$_3$C−); not observed N≡*C* and B(C$_6$F$_5$)$_3$ (ipso-*C*). ^{11}B NMR (64.2 MHz, benzene-d_6): δ = −21.8 ($\nu_{1/2}$ = 10 ± 1 Hz). ^{19}F NMR (282.4 MHz, benzene-d_6): δ = −134.8 (m, 2F, (m-*F*)), −155.3 (t, $^3J_{FF}$ = 21 Hz, 1F, (p-*F*)), −162.9 (m, 2F, (o-*F*)). IR (KBr): $\tilde{\nu}$ = 2310 (N≡C) cm^{-1}. X-ray crystal structure analysis of **3a**: formula $C_{23}H_9NBF_{15}$, M = 595.12, colorless, 0.40 × 0.30 × 0.10 mm, a = 9.345(2) Å, b = 11.545(2) Å, c = 12.053(2) Å, α = 61.45(1)°, β = 85.75(1)°, γ = 88.23(1)°, V = 1139.1(4) Å^3, ρ_{calc} = 1.735 g cm^{-3}, μ = 1.88 cm^{-1}, empirical absorption correction via ψ scan data ($0.945 \le C \le 0.999$), $Z = 2$, triclinic, space group $P\bar{1}$ (No. 2), $\lambda = 0.710\,73$ Å, $T = 223$ K, $\omega/2\theta$ scans, 4849 reflections collected ($\pm h, +k, \pm l$), [(sin θ)/λ] = 0.62 Å^{-1}, 4609 independent and 2493 observed reflections [$I \ge 2\sigma(I)$], 364 refined parameters, $R = 0.041$, wR2 = 0.095, max. residual electron density 0.20 (−0.28) e·Å^{-3}, hydrogens calculated and riding.

Tris(pentafluorophenyl)borane−1,1,3,3-Tetramethylbutylisocyanide, Complex (3b). Tris(pentafluorophenyl)borane (1.00 g, 1.95 mmol) and 300 mg (2.15 mmol) of 1,1,3,3-tetramethylbutylisocyanide give the product **3b**. Yield of **3b**: 1.25 g (98%), mp 129 °C (DSC). $C_{27}H_{17}BF_{15}N$ (651.2): calcd C 49.80, H 2.63, N 2.15; found C 49.64, H 2.48, N 2.10. ^{1}H NMR (200.1 MHz, benzene-d_6): δ = 1.04 (s, 2H, −CH_2−), 0.89 (s, 6H, (CH_3)$_2$C−), 0.57 (s, 9H, (CH_3)$_3$C−). ^{13}C NMR (50.3 MHz, benzene-d_6): δ = 148.5 (dm, $^1J_{CF}$ = 241 Hz, B(C$_6$F$_5$)$_3$ (o-*C*)), 140.9 (dm, $^1J_{CF}$ = 253 Hz, B(C$_6$F$_5$)$_3$ (p-*C*)), 137.8 (dm, $^1J_{CF}$ = 255 Hz, B(C$_6$F$_5$)$_3$ (m-*C*)), 63.8 ((CH$_3$)$_2$*C*−), 52.0 (−*C*H$_2$−), 31.0 ((CH$_3$)$_3$*C*−), 29.9 ((*C*H$_3$)$_3$C−), 28.8 ((*C*H$_3$)$_2$C−); not observed N≡*C* and B(C$_6$F$_5$)$_3$ (ipso-*C*). ^{11}B NMR (64.2 MHz, benzene-d_6): δ = −21.7 (ν_- = 12 ± 1 Hz). ^{19}F NMR (282.4 MHz, benzene-d_6): δ = −133.2 (m, 2F, (m-*F*)), −155.3 (t, $^3J_{FF}$ = 21 Hz, 1F, (p-*F*)), −162.9 (m, 2F, (o-*F*)). IR (KBr): $\tilde{\nu}$ = 2301 (N≡C) cm^{-1}. X-ray crystal structure analysis of **3b**: formula $C_{27}H_{17}NBF_{15}$, M = 651.23, colorless, 0.30 × 0.20 × 0.10 mm, a = 9.018(1) Å, b = 10.800(1) Å, c = 14.871(2) Å, α = 77.38(1)°, β = 76.53(1)°, γ = 73.16(1)°, V = 1330.3(3) Å^3, ρ_{calc} = 1.626 g cm^{-3}, μ = 1.68 cm^{-1}, empirical absorption correction via ψ scan data ($0.943 \le C \le 0.999$), $Z = 2$, triclinic, space group $P\bar{1}$ (No. 2), $\lambda = 0.710\,73$ Å, $T = 223$ K, $\omega/2\theta$ scans, 5704 reflections collected ($\pm h, -k, \pm l$), [(sin θ)/λ] = 0.62 Å^{-1}, 5403 independent and 2655 observed reflections [$I \ge 2\,\sigma(I)$], 402 refined parameters, $R = 0.046$, wR2 = 0.098, max. residual electron density 0.20 (−0.24) e·Å^{-3}, hydrogens calculated and riding.

Tris(pentafluorophenyl)borane−2,6-Dimethylphenylisocyanide, Complex (3c). Tris(pentafluorophenyl)borane (1.00 g, 1.95 mmol) and 280 mg (2.13 mmol) of 2,6-dimethylphenylisocyanide give the product **3c**. Yield of **3c**: 1.19 g (95%), mp 130 °C (DSC). $C_{27}H_9BF_{15}N$ (643.2): calcd C 50.43, H 1.41, N 2.18; found C 50.59, H 1.70, N 2.31. ^{1}H NMR (200.1 MHz, benzene-d_6): δ = 6.63 (d, 1H, $^3J_{HH}$ = 7.55 Hz, (p-*H*)), 6.36 (d, 2H, $^3J_{HH}$ = 7.55 Hz, Ph (m-*H*)), 1.80 (s, 6H, CH_3). ^{13}C NMR (50.3 MHz, benzene-d_6): δ = 148.5 (dm, $^1J_{CF}$ = 247 Hz, B(C$_6$F$_5$)$_3$ (o-*C*)), 141 (dm, $^1J_{CF}$ = 252 Hz, B(C$_6$F$_5$)$_3$ (p-*C*)), 137.8 (dm, $^1J_{CF}$ = 253 Hz, B(C$_6$F$_5$)$_3$ (m-*C*)), 132.3 (Ph (p-*C*)), 137.4 (Ph (o-*C*)), 128.7 (Ph (m-*C*)), 17.2 (*C*H$_3$); not observed N≡*C*, Ph (ispo-*C*) and B(C$_6$F$_5$)$_3$ (ipso-*C*). ^{11}B NMR (64.2 MHz, benzene-d_6): δ = −21.0 ($\nu_{1/2}$ = 14 ± 1 Hz). ^{19}F NMR (282.4 MHz, benzene-d_6): δ = −132.3 (m, 2F, (m-*F*)), −155.2 (t, $^3J_{FF}$ = 21 Hz, 1F, (p-*F*)), −162.7 (m, 2F, (o-*F*)). IR (KBr): $\tilde{\nu}$ = 2275 (N≡C) cm^{-1}.

Tris(pentafluorophenyl)borane−Triphenylphosphine, Complex 6. A solution of 560 mg (2.14 mmol) of triphenylphoshine in 50 mL of pentane was added dropwise to a solution of 1.00 g (1.95 mmol) of tris(pentafluorophenyl)-borane in the same volume of pentane. The reaction mixture was refluxed until the product precipitated. After further stirring for 1 h at room temperature, the solid product was isolated by filtration, washed twice with 20 mL of pentane, and dried in vacuo. The product was obtained as a colorless powder. Yield of **6**: 1.24 g (82%), mp 203 °C (DSC, decomp.). $C_{36}H_{15}BF_{15}P$ (774.3): calcd C 55.84, H 1.95; found C 55.19, H 1.97. ^{1}H NMR (200.1 MHz, benzene-d_6): δ = 7.33−7.24 and 7.10−7.05 (2m, 15H, PPh$_3$). ^{13}C NMR (50.3 MHz, benzene-d_6): δ = 148.8 (dm, $^1J_{CF}$ = 253 Hz, B(C$_6$F$_5$)$_3$ (o-*C*)), 140.8 (dm, $^1J_{CF}$ = 262 Hz, B(C$_6$F$_5$)$_3$ (p-*C*)), 137.2 (dm, $^1J_{CF}$ = 247 Hz, B(C$_6$F$_5$)$_3$ (m-*C*)), 133.3 (d, $^3J_{PC}$ = 10 Hz, Ph (m-*C*)), 130.2 (d, $^2J_{PC}$ = 13 Hz, Ph (o-*C*)), 128.8 (d, $^4J_{PC}$ = 7 Hz, Ph (p-*C*)); not observed Ph$_3$P (ipso-*C*) and B(C$_6$F$_5$)$_3$ (ipso-*C*). ^{11}B NMR (64.2 MHz, benzene-d_6): δ = −2.5 ($\nu_{1/2}$ = 110 ± 10 Hz). ^{31}P NMR (81.0 MHz, benzene-d_6): δ = −5.2. ^{19}F NMR (282.4 MHz, benzene-d_6): δ = −134.8 (m, 2F, (m-*F*)), −157.3 (t, $^3J_{FF}$ = 21 Hz, 1F, (p-*F*)), −164.4 (m, 2F, (o-*F*)). X-ray crystal structure analysis of **6**: formula $C_{36}H_{15}BF_{15}P$, M = 774.26, colorless, 0.30 × 0.25 × 0.10 mm, a = 32.194(3) Å, b = 8.655(1) Å, c = 22.673-(2) Å, β = 105.52(1)°, V = 6087.2(11) Å^3, ρ_{calc} = 1.690 g cm^{-3}, μ = 2.12 cm^{-1}, empirical absorption correction via ψ scan data ($0.983 \le C \le 0.992$), $Z = 8$, monoclinic, space group $C2/c$ (No. 15), $\lambda = 0.710\,73$ Å, $T = 223$ K, $\omega/2\theta$ scans, 3682 reflections collected ($+h, +k, \pm l$), [(sin θ)/λ] = 0.54 Å^{-1}, 3611 independent and 1979 observed reflections [$I \ge 2\ \sigma(I)$], 478 refined parameters, $R = 0.040$, wR2 = 0.077, max. residual electron density 0.26 (−0.30) e·Å^{-3}, hydrogens calculated and riding.

Acknowledgment. Financial support from the Swiss National Science Foundation SNSF (H.B.) and from the Fonds der Chemischen Industrie and the Deutsche Forschungsgemeinschaft (G.E.) is gratefully acknowledged.

Supporting Information Available: Additional material concerning the X-ray structure analyses of the complexes **1a**, **1c**, **3a**, **3b**, and **6** including complete listings of X-ray parameters, bond lengths and angles, and positional and thermal parameters, and a listing of calculated total bonding energies. This material is available free of charge via the Internet at http://pubs.acs.org.

OM981033E